Hot debris dust around HD 106797

Hideaki Fujiwara[1], Takuya Yamashita[2], Daisuke Ishihara[3], Takashi Onaka[1], Hirokazu Kataza[3], Takafumi Ootsubo[3], Misato Fukagawa[4], Jonathan P. Marshall[5], Hiroshi Murakami[3], Takao Nakagawa[3], Takanori Hirao[3], Keigo Enya[3], and Glenn J. White[5,6]

ABSTRACT

Photometry of the A0 V main-sequence star HD 106797 with *AKARI* and Gemini/T-ReCS is used to detect excess emission over the expected stellar photospheric emission between 10 and 20 μm, which is best attributed to hot circumstellar debris dust surrounding the star. The temperature of the debris dust is derived as $T_{\rm d} \sim 190$ K by assuming that the excess emission is approximated by a single temperature blackbody. The derived temperature suggests that the inner radius of the debris disk is ~ 14 AU. The fractional luminosity of the debris disk is 1000 times brighter than that of our own zodiacal cloud. The existence of such a large amount of hot dust around HD 106797 cannot be accounted for by a simple model of the steady state evolution of a debris disk due to collisions, and it is likely that transient events play a significant role. Our data also show a narrow spectral feature between 11 and 12 μm attributable to crystalline silicates, suggesting that dust heating has occurred during the formation and evolution of the debris disk of HD 106797.

Subject headings: circumstellar matter — planetary systems: formation — infrared: stars — stars: individual (HD 106797)

1. Introduction

Infrared Astronomical Satellite (*IRAS*) detected a number of main-sequence stars that show infrared excesses above their expected photospheric emission (e.g. Aumann et al. 1984; Rhee et al. 2007). These infrared excesses are thought to originate from second generation dust grains formed as a consequence of the collision of planetesimals, or the destruction of cometary objects (e.g. Backman & Paresce 1993; Lecavelier Des Etangs et al. 1996).

Most of the known debris disks only show excesses at wavelengths longer than 25 μm. The excess comes from the thermal emission of dust grains with low temperatures ($T_{\rm dust} \sim 100$ K) that exist far from the central star. To date, little is known about the properties of the debris disk material located close to the star, which has a more direct link to the formation of terrestrial planets than the low temperature debris (Meyer et al. 2008). The recent availability of high-sensitivity surveys at $10 - 20$ μm allows the properties of this inner debris disk material to be measured. In this Letter, we report observations obtained with the mid-infrared (MIR) all-sky survey made by the *AKARI* satellite (Murakami et al. 2007).

AKARI is a Japanese infrared satellite mostly dedicated to an infrared all-sky survey, which was

[1]Department of Astronomy, School of Science, University of Tokyo, Bunkyo-ku, Tokyo 113-0033, Japan; fujiwara@astron.s.u-tokyo.ac.jp

[2]National Astronomical Observatory of Japan, 2-21-1 Osawa, Mitaka, Tokyo 181-0015, Japan

[3]Institute of Space and Astronautical Science, Japan Aerospace Exploration Agency, 3-1-1 Yoshinodai, Sagamihara, Kanagawa 229-8510, Japan

[4]Graduate School of Science, Osaka University, 1-1 Machikaneyama, Toyonaka 560-0043, Osaka, Japan

[5]Department of Physics and Astronomy, The Open University, Walton Hall, Milton Keynes, MK7 6AA, England

[6]Space Science & Technology Department, The Rutherford Appleton Laboratory, Chilton, Didcot, Oxfordshire OX11 0QX, England

launched in February 2006. The MIR all-sky survey was performed using 9 and 18 μm broad band filters with the InfraRed Camera (IRC) onboard *AKARI* until August 2008 (Ishihara et al. 2006). Since the peak of the thermal emission from hot dust grains with $T_{\rm dust} \gtrsim 200$ K comes to around $10 - 20$ μm, the *AKARI*/IRC all-sky survey data are a powerful tool to search for hot debris disks which should be connected with the formation process of terrestrial planets.

Here we report a discovery of significant 18 μm excess towards the A0 V main-sequence star HD 106797 from the *AKARI*/IRC all-sky survey data. The distance to the star from the Sun is measured as $d = 96 \pm 3$ pc based on *Hipparcos* observations (van Leeuwen 2007). In addition, we discover significant excess emission at 11.7 and 12.4 μm by narrow band photometric observations with the Gemini/T-ReCS.

In this Letter, we show the spectral energy distribution (SED) in the MIR region of HD 106797 and discuss the spatial distribution and mineralogical properties of the hot debris dust around HD 106797.

2. Observations and Data Reduction

2.1. *AKARI*/IRC all-sky survey

The S9W (9 μm) and L18W (18 μm) images of HD 106797 were taken as part of the All-Sky Survey observations. The star was observed on 2006 August 6, 2007 February 1, 2, August 6 and 7. In the All-Sky Survey, the IRC was operated in the scan mode with the scan speed of $215''$ sec^{-1} and the data sampling time of 0.044 sec, which provided a spatial resolution of $\sim 10''$ along the scan direction. The spatial resolution along the cross-scan direction was $\sim 10''$ (Ishihara et al. 2006). The All-Sky Survey data were reduced using the standard *AKARI* pipeline software version 061210. The data from the three periods were median combined. The 5-σ sensitivity for a point source per scan is estimated to be 50 mJy in the S9W band and 120 mJy in the L18W band, and the absolute uncertainty in flux density is 7 % for the S9W band and 15 % for the L18W band at present. The spatial resolution is improved to $5''$ in the both bands by combining the dithered data of multiple observations in the pipeline. The absolute position accuracy is estimated to be $5''$ (Ishihara et al. 2006). The fluxes at the three periods agree with each other within the uncertainty, indicating no significant variations in the flux. HD 106797 was selected as a probable candidate of debris disk with 18 μm excess from a preliminary search for debris disks based on the *AKARI*/IRC All-Sky Survey data.

2.2. Ground-based follow-up observations with Gemini/T-ReCS

HD 106797 was observed with the T-ReCS (Telesco et al. 1998), mounted on the 8 m Gemini South Telescope on 2007 June 10 and 12. Imaging observations in the 8.8 micron ($\Delta\lambda = 0.8$ μm), 9.7 μm ($\Delta\lambda = 0.9$ μm), 10.4 μm ($\Delta\lambda = 1.0$ μm), 11.7 μm ($\Delta\lambda = 1.1$ μm), 12.3 μm ($\Delta\lambda = 1.2$ μm), and 18.3 μm ($\Delta\lambda = 1.5$ μm) bands were carried out. The pixel scale was $0\farcs09$ pixel^{-1}. To cancel out the background radiation, the secondary mirror chopping and the telescope nodding method were used. We used a standard star (HD 110458) from Cohen et al. (1999) as a flux calibrator and reference point-spread functions (PSFs) were derived by observations. We observed the standard star before or after the observations of the target star in the same manner. The observation parameters are summarized in Table 1.

For the data reduction, we used our own reduction tools and IRAF. The standard chop-nod pair subtraction and the shift-and-add method in the unit of 0.1 pixel were employed. We applied air mass correction by estimating the difference in atmospheric absorption using the ATRAN software (Lord 1992). The difference in the air mass between the object and the standard star was quite small ($\lesssim 0.1$) and thus the correction factor in each band is less than 5 %.

3. Results

3.1. Spectral Energy Distribution

The observed flux densities of HD 106797 in all bands are shown in Table 2. The photospheric flux densities are estimated from the Kurucz model of A0 stars with the effective temperature of $T_{\rm eff} = 9750$ K and the surface gravity of $\log g = +4.0$ (Kurucz 1992) fitted to the 2MASS $K_{\rm s}$-band photometry of the star and also shown in Table 2. The SED of the star in the near-infrared (NIR) and MIR regions is shown in Figure 1.

No significant excess emission in the *AKARI*/IRC S9W band is found. The 18 μm flux densities derived with *AKARI*/IRC and Gemini/T-ReCS are in agreement with each other. Although *AKARI* data with a beam size of ~ 5 $''$ might be contaminated by other nearby sources, we did not find any other infrared sources besides HD 106797 in the field of view of T-ReCS ($28\farcs8 \times 21\farcs6$). Therefore it can securely be concluded that the 18 μm excess towards HD 106797 is associated with the star.

In addition to the 18 μm excess, T-ReCS narrow band photometry also indicates excess emission at 11.7 and 12.3 μm towards HD 106797, suggesting that there are hot ($T_{\rm d} \gtrsim 200$ K) debris dust grains around HD 106797. We can also see a bump around 11.7 μm in the SED, suggesting the presence of a silicate dust feature in the excess emission.

To make an initial estimation of the dust temperature and the luminosity, we performed a fit with the SED model of

$$F_{\nu,\rm model}(\lambda) = \mathrm{Kurucz}(T_{\rm eff} = 9750\ \mathrm{K}) + \mathrm{BB}_\nu(\lambda, T_{\rm d}), \quad (1)$$

where Kurucz($T_{\rm eff} = 9750$ K) is the Kurucz model of A0 stars (Kurucz 1992) for the photospheric contribution and $\mathrm{BB}_\nu(\lambda, T_{\rm d})$ is a blackbody of a single temperature $T_{\rm d}$ for excess emission. The Kurucz template is scaled to fit the 2MASS $K_{\rm s}$-band flux because interstellar extinction is smaller in the $K_{\rm s}$-band than in the J- and H-bands. The stellar luminosity is derived as 42.4 $L_\odot$. A blackbody of $T_{\rm d} = 192$ K gives the best fit to the observed SED in the *N*- and *Q*-bands. The dust luminosity is derived as 0.00819 $L_\odot$. The dust temperature is appropriate for dust grains at a distance of 13.7 AU from the central A0 V star when the dust grains are assumed as blackbody that follows the relation of $d \propto T_{\rm d}^{-2}$. In other words, the inner radius of the debris disk around HD 106797 is ~ 14 AU. We cannot estimate the degree of extension of the debris disk only from the SED since far-infrared (FIR) photometric data are not available.

Here we performed a fit to the observed excess emission with a simple SED model of a blackbody of a single temperature. We should note that the flux densities of the best-fit SED model at $\lambda \lesssim 10.4$ μm are larger than the T-ReCS observations. However this problem may be solved by considering dust species whose emissivity is small at $\lambda \lesssim 10.4$ μm as a carrier of the excess emission. We discuss the possible carrier of the excess emission in Section 4.1.

3.2. Radial Profile

We compare the peak-normalized azimuthally averaged radial profile of HD 106797 at 11.7 μm with the PSF standard by using the T-ReCS data to investigate the spatial distribution of the debris dust around HD 106797. The debris disk is unresolved and no significant structures are seen in the radial profiles in all bands. Since the FWHM of the PSF standard at 11.7 μm is $0\farcs43$, the size of the debris disk around HD 106797 is less than 41 AU at the distance of the star ($d = 96$ pc), which is consistent with the inner radius of the disk estimated from the SED.

4. Discussion

4.1. Features in the *N*-band

The excess flux densities derived by subtraction of the photospheric contribution are shown in Figure 2. The IRC/S9W excess flux density is in agreement with the T-ReCS data at $\lambda \lesssim 10.4$ μm. However, the excess flux densities at 11.7 and 12.3 μm are significantly larger than those at $\lambda \lesssim 10.4$ μm, suggesting the dust emission has a feature around $11 - 12$ μm. Since the IRC/S9W band does not cover wavelengths $\gtrsim 11.6$ μm, the 11.7 and 12.3 μm data are not incompatible with the IRC/S9W flux.

To identify the possible carrier of the feature, we perform additional fits for the excess emission with the SED model of

$$F_{\rm excess,\nu}(\lambda) = a\kappa(\lambda)\mathrm{BB}_\nu(\lambda, T_{\rm d}), \quad (2)$$

where $\kappa(\lambda)$ is mass absorption coefficient of dust and a is scaling factor. We consider the mass absorption coefficients of four kinds of silicates, 0.1 μm- and 2.0 μm-sized amorphous olivine (Dorschner et al. 1995), crystalline forsterite, and crystalline fayalite (Koike et al. 2003). The best-fit result for each dust species is overlaid on the observed data in Figure 2. Amorphous olivine particles of 0.1 μm size show a triangular feature with a peak at 9.7 μm and cannot account for the observed narrow feature around $11 - 12$ μm. Amorphous olivine particles of 2.0 μm size give a

better fit than those of 0.1 μm size. However they produce extra emission at $\lambda \lesssim 10.4$ μm, and thus they also cannot account for the observations very well. In contrast, crystalline forsterite and fayalite show the strongest feature at $11.3 - 11.4$ μm in the *N*-band (Koike et al. 2003), which may account for the observed narrow feature. Polycyclic aromatic hydrocarbons (PAHs) also show a significant feature at 11.3 μm (Allamandola et al. 1989). However PAHs commonly show a stronger feature at 7.7 μm than that at 11.3 μm. We cannot see any significant excess around 8 μm toward HD 106797, and thus PAHs are ruled out as a carrier of $11 - 12$ μm feature. Crystalline forsterite and fayalite are likelier carriers of the $11 - 12$ μm feature than amorphous silicate and PAHs. The resultant χ^2_ν-values by the fits suggest that fayalite is more plausible. The dust temperatures derived from the fits with crystalline forsterite and fayalite are 190 and 174 K, respectively. Therefore, we conclude that the presence of hot debris dust around the star is secure. The $11.3 - 11.4$ μm fine structure is discovered towards some debris disks in MIR spectra obtained with the Infrared Spectrograph onboard *Spitzer* (Beichman et al. 2005; Chen et al. 2006) and the COMICS onboard the Subaru Telescope (Honda et al. 2004), which is attributed to crystalline forsterite or fayalite. We note that the observed *N*-band feature towards HD 106797 is not accounted for completely by crystalline forsterite nor fayalite. The observed feature seems to be located at slightly longer wavelengths than the $11.3 - 11.4$ μm peak of the crystalline forsterite or fayalite, suggesting a possible existence of other species of dust grains around HD 106797.

4.2. Origin of hot dust

The fractional luminosity $L_{\rm dust}/L_{\rm star}$ of HD 106797 is derived as $\sim 1.93 \times 10^{-4}$ by integrating the best-fit SED model of the star and the excess from 0.01 to 1000 μm. The fractional luminosity of our own zodiacal cloud is estimated as an order of $\sim 10^{-7}$ (Backman & Paresce 1993). Thus the debris disk around HD 106797 is 1000 times brighter than our own zodiacal cloud. Wyatt et al. (2007) develop a simple model for the steady state evolution of debris disks due to collisions based on Wyatt & Dent (2002). The model indicates that a fractional luminosity larger than 10^{-4} is obtained only in the stage less than a few Myr for A0 V stars. Although the age of HD 106797 is unknown, the star is thought to be older than 10 Myr since the star is not labeled as an emission line star in the Tycho-2 spectral type catalog (Wright et al. 2003), which is one of the strong indicators of young stars. Therefore the existence of a large amount of hot dust around HD 106797 cannot be accounted for by a simple steady state model. The system must be undergoing some kind of transient events. For example, the origin for this transient dust may be accounted for by a dynamical instability that scatters planetesimals inward from a more distant planetesimal belt. Then the dust is released from the planetesimals in collisions and sublimation. The transient event is akin to the late heavy bombardment (LHB) in the solar system, a cataclysmic event 700 Myr after the initial formation of the solar system, as implied by the Moon's cratering record (e.g. Hartmann et al. 2000).

As discussed in a previous section, HD 106797 shows a $11-12$ μm feature that may originate from crystalline silicate. In the interstellar medium, silicates are mostly amorphous (Kemper et al. 2004). Crystallization of silicates requires heating to a temperature higher than 800 K (Hallenbeck et al. 2000). How were high temperature products such as crystalline silicate produced in the region at which dust temperature is estimated to be less than 300 K? This question is akin to the crystalline silicate problem of comets in the solar system. Several models have been proposed to account for the problem. Bockelée-Morvan et al. (2002) propose a model in which silicate dust particles heated by radiation from the central star and crystallized at the central region of the disk are transported outward to the cold region of the disk by a turbulent flow or an X-wind. On the other hand, Harker & Desch (2002) propose a model in which silicate dust particles in the cold region of the outer disk are heated by shock wave and crystallized in situ. Both models are able to account for the distributions of crystalline silicate in a few tens of AU from the central star although it is still unclear which mechanism is the most effective. Resolving the radial distributions of every dust species in the debris disk of HD 106797 with future spectroscopy with high spatial resolution should give us an insight into the problem.

While more than one hundred debris disks

with large 60 μm excess have been discovered (Rhee et al. 2007), only seven debris disks with large 10 μm excess (fractional luminosity $\gtrsim 0.5$ at 10 μm) have been reported so far (β Pic, HIP 8920, HD 113766, HR 7012, η Crv, HD 145263, and HD 202406; Telesco et al. 2005; Song et al. 2005; Chen et al. 2006; Smith et al. 2008). Therefore debris disks with large 10 μm excess are so far rare. All of the 10 μm excesses are thought to attribute to hot dust of $T_{\rm d} \gtrsim 200$ K. β Pic also shows large far-infrared excess attributable to abundant cold dust (Backman et al. 1992).

In should be noted that in spite of the large MIR excess, HD 106797 is not detected in the FIR region either by the Far-Infrared Surveyor (FIS) onboard *AKARI* (J. P. Marshall, private communication) or by the *IRAS* observations. Both of the the FIS/WIDE-S ($60-110$ μm) and the *IRAS* 60 μm detection limits are about 1.5 Jy. Thus HD 106797 may be an example of a debris disk source, in which hot dust is very abundant while Kuiper-belt-analog cold dust is not. The present discovery of the 10 μm excess towards HD 106797 suggests a presence of the new kind of debris disk around main-sequence stars.

Most of the reported debris disks with large 10 μm excess including HD 106796 show fine structures in the *N*-band attributable to crystalline silicates (Knacke et al. 1993; Song et al. 2005; Chen et al. 2006; Honda et al. 2004) except for HD 202406, whose MIR measurements with a wavelength resolution high enough to discuss the fine structure are not available. We speculate that transient events like the LHB tend to cause dust heating and generate crystalline silicates efficiently.

This research is based on observations with the *AKARI*, a JAXA project with the participation of ESA. This research is also based on data collected at the Gemini Observatory, through the time exchange programs with the Subaru Telescope, which is operated by the National Astronomical Observatory of Japan. We appreciate the support from the Gemini Observatory staff. We thank Chiyoe Koike and Hiroki Chihara for providing us with crystalline silicate spectra and their useful comments. We also thank the anonymous referee, Aki Takigawa, Shogo Tachibana, and Alexander V. Krivov for their useful comments and suggestions. This research was supported by the MEXT, "Development of Extrasolar Planetary Science," and the UK science and Technology Facilities Council. H.F. is financially supported by the Japan Society for the Promotion of Science.

Facilities: *AKARI* (ISAS/JAXA), Gemini-South (AURA).

REFERENCES

Allamandola, L. J., Tielens, A. G. G. M., & Barker, J. R. 1989, ApJS, 71, 733

Aumann, H. H., et al. 1984, ApJ, 278, L23

Backman, D. E., & Paresce, F. 1993, Protostars and Planets III, 1253

Backman, D. E., Witteborn, F. C., & Gillett, F. C. 1992, ApJ, 385, 670

Beichman, C. A., et al. 2005, ApJ, 626, 1061

Bockelée-Morvan, D., Gautier, D., Hersant, F., Huré, J.-M., & Robert, F. 2002, A&A, 384, 1107

Chen, C. H., et al. 2006, ApJS, 166, 351

Cohen, M., Walker, R. G., Carter, B., Hammersley, P., Kidger, M., & Noguchi, K. 1999, AJ, 117, 1864

Dorschner, J., Begemann, B., Henning, T., Jaeger, C., & Mutschke, H. 1995, A&A, 300, 503

Hallenbeck, S. L., Nuth, J. A., III, & Nelson, R. N. 2000, ApJ, 535, 247

Harker, D. E., & Desch, S. J. 2002, ApJ, 565, L109

Hartmann, W. K., Ryder, G., Dones, L., & Grinspoon, D. 2000, Origin of the earth and moon, edited by R.M. Canup and K. Righter and 69 collaborating authors. Tucson: University of Arizona Press., p.493-512, 493

Honda, M., et al. 2004, ApJ, 610, L49

Ishihara, D., et al. 2006, PASP, 118, 324

Kemper, F., Vriend, W. J., & Tielens, A. G. G. M. 2004, ApJ, 609, 826

Knacke, R. F., Fajardo-Acosta, S. B., Telesco, C. M., Hackwell, J. A., Lynch, D. K., & Russell, R. W. 1993, ApJ, 418, 440

Koike, C., Chihara, H., Tsuchiyama, A., Suto, H., Sogawa, H., & Okuda, H. 2003, A&A, 399, 1101

Kurucz, R. L. 1992, The Stellar Populations of Galaxies, 149, 225

Lecavelier Des Etangs, A., Vidal-Madjar, A., & Ferlet, R. 1996, A&A, 307, 542

Lord, S. D. 1992, A New Software Tool for Computing Earthfs Atmospheric Transmission of Near- and Far-Infrared Radiation (NASA Tech. Memo 103957; Washington, DC: NASA)

Meyer, M. R., et al. 2008, ApJ, 673, L181

Murakami, H., et al. 2007, PASJ, 59, 369

Rhee, J. H., Song, I., Zuckerman, B., & McElwain, M. 2007, ApJ, 660, 1556

Smith, R., Wyatt, M. C., & Dent, W. R. F. 2008, A&A, 485, 897

Song, I., Zuckerman, B., Weinberger, A. J., & Becklin, E. E. 2005, Nature, 436, 363

Telesco, C. M., Pina, R. K., Hanna, K. T., Julian, J. A., Hon, D. B., & Kisko, T. M. 1998, Proc. SPIE, 3354, 534

Telesco, C. M., et al. 2005, Nature, 433, 133

van Leeuwen, F. 2007, Astrophysics and Space Science Library, 350,

Wright, C. O., Egan, M. P., Kraemer, K. E., & Price, S. D. 2003, AJ, 125, 359

Wyatt, M. C., & Dent, W. R. F. 2002, MNRAS, 334, 589

Wyatt, M. C., Smith, R., Greaves, J. S., Beichman, C. A., Bryden, G., & Lisse, C. M. 2007, ApJ, 658, 569

This 2-column preprint was prepared with the AAS LaTeX macros v5.2.

Table 1: Summary of Gemini/T-ReCS observations.

Object	Filter (μm)	Date & Time (UT)	Integration (s)	Air Mass	Comment
HD 106797	18.3	10 June 2008 04:18:04	811	1.79	···
HD 110458	18.3	10 June 2008 05:09:19	116	1.91	Standard
HD 106797	12.3	12 June 2008 03:10:34	174	1.50	···
HD 106797	11.7	12 June 2008 03:20:49	116	1.52	···
HD 106797	10.4	12 June 2008 03:27:48	58	1.54	···
HD 106797	9.7	12 June 2008 03:31:32	174	1.56	···
HD 106797	8.8	12 June 2008 03:41:48	58	1.59	···
HD 110458	8.8	12 June 2008 03:48:42	58	1.45	Standard
HD 110458	9.7	12 June 2008 03:52:26	58	1.46	Standard
HD 110458	10.4	12 June 2008 03:56:10	58	1.48	Standard
HD 110458	11.7	12 June 2008 03:59:55	58	1.50	Standard
HD 110458	12.3	12 June 2008 04:03:39	58	1.52	Standard

Table 2: Infrared Photometry of HD 106797.

λ (μm)	F_ν (mJy)	Instrument	Photosphere[a] (mJy)	Significance, χ[b]
8.8	201 ± 20	T-ReCS	206	-0.3
9	216 ± 15	IRC	214	0.1
9.7	165 ± 17	T-ReCS	166	-0.1
10.4	159 ± 15	T-ReCS	145	0.9
11.7	180 ± 14	T-ReCS	115	4.6
12.4	160 ± 13	T-ReCS	104	4.2
18	128 ± 19	IRC	55	3.8
18.3	119 ± 59	T-ReCS	47	1.2

[a] From Kurucz model to fitted to 2MASS Ks-band data.

[b] χ = (Observed − Kurucz)/noise.

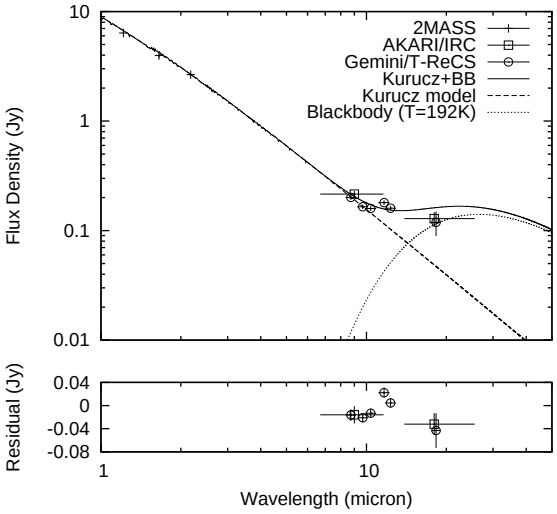

Fig. 1.— *Top*: The NIR and MIR SED of HD 106797 and the results of SED fitting with a model which is consistent with a Kurucz model for photospheric contribution and a blackbody of a single temperature $T_{\rm d} = 192$ K for dust emission. Open squares and circles indicate the photometry with the *AKARI*/IRC and Gemini/T-ReCS, repectively. Solid, dashed and dotted lines indicate the total SED, photospheric contribution, and dust emission of the blackbody model, respectively. *Bottom*: The residuals subtracted by the best-fit SED model in the MIR region.

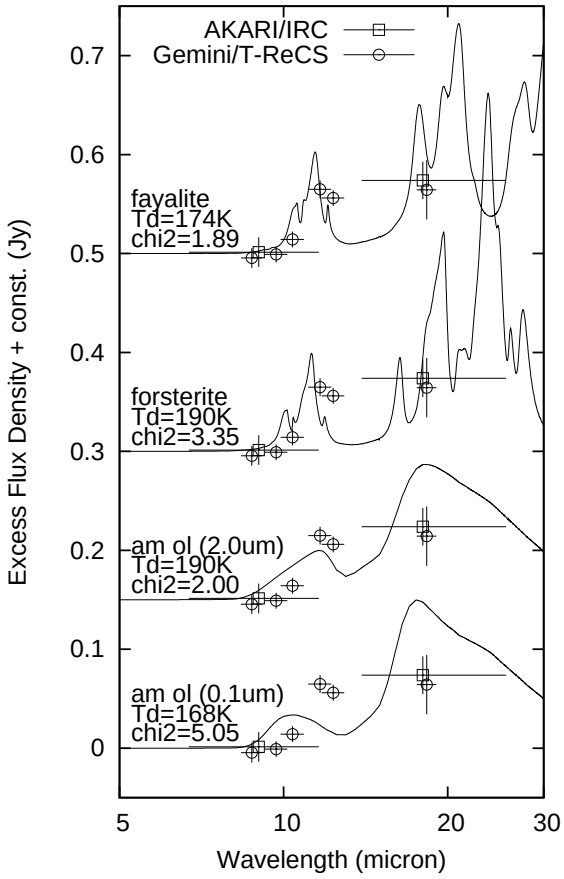

Fig. 2.— The excess flux densities together with model fit results of various dust species. Open squares and circles indicate the residual flux densities with the *AKARI*/IRC and Gemini/T-ReCS, repectively. The solid line indicate the best-fit result for the each dust species (0.1 μm- and 2.0 μm-sized amorphous olivine (Dorschner et al. 1995), crystalline forsterite (Koike et al. 2003), and crystalline fayalite (Koike et al. 2003)). The resultant best-fit dust temperature and χ^2_ν-value for each dust species are also shown. As seen in this figure, crystalline fayalite provides the best-fit result.